

# PASSENGER VEHICLE STRUCTURAL RESPONSE IN A DYNAMIC ROLLOVER TEST

Garrett A. Mattos

Raphael H. Grzebieta

Mike R. Bambach

Andrew S. McIntosh

Transport and Road Safety (TARS) Research

University of New South Wales

Australia

Paper Number 13-0067

## ABSTRACT

The structural performance of a vehicle has been shown to be associated with the likelihood of sustaining serious injury in passenger vehicle rollover crashes. With increasing interest in implementing interior safety features, such as side curtain airbags, to mitigate injury during rollover it is important to understand the response of the vehicle structure onto which many of these devices are attached. Further, research is ongoing to determine the feasibility of using a dynamic rollover test device, such as the Jordan Rollover System (JRS), to accurately assess a vehicle's ability to protect occupants in rollover crashes. This research requires an understanding of the performance of the tests performed on such a system. The objective of this paper is to investigate the response of the vehicle structure, as tested on the JRS, with specific focus on the relationship between the dynamic and residual roof intrusion. This paper will also investigate the kinematic response of the vehicle and how it is related to roof performance and test conditions.

## INTRODUCTION

The structural performance (maximum/residual roof intrusion and intrusion speed) of a vehicle in dynamic rollover and quasi-static roof strength tests has been shown to be significantly associated with its real world rollover injury rate [1-3]. Differences in vehicle kinematics during dolly rollover tests have been observed for the same vehicle shape with different roof strengths [4, 5]. The Jordan Rollover System (JRS) is currently the test device of choice in an effort to assess the viability of a dynamic rollover test for use in compliance and/or vehicle performance rating tests [6]. In this effort it is important to understand how vehicles perform on the system as well as how the test conditions affect that performance.

## METHODS

Dynamic rollover tests of forty-eight passenger vehicles conducted over the past 5 years on the Jordan Rollover System (JRS) at the Center for Injury Research (CFIR) were used to study various measures of vehicle structural and kinematic

performance. The test data was provided to the authors by the CFIR.

The JRS, Figure 1, is a dynamic rollover test device that has been proven to provide a repeatable and valid representation of the interaction between the roadbed and roof of the vehicle during a lateral tripped rollover [7-10]. The JRS suspends a vehicle, which is free to spin about its longitudinal axis, above a track with a moving roadbed. The vehicle can be positioned with predetermined pitch, yaw, and drop height. At the start of the test the vehicle is rotated at a prescribed angular velocity and is dropped to impact the moving roadbed at the designated roll and pitch angle. The terms near and far are used to describe the side of the vehicle that impacts the road first and last, respectively.

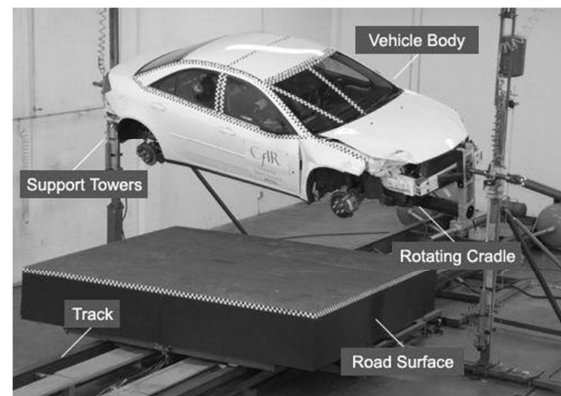


Figure 1. Jordan rollover system.

The JRS measures roadbed speed, vertical and lateral road loads, vehicle angular velocity, and vehicle vertical motion at the front and rear towers. With this information the energy of the entire system can be tracked throughout each test using the basic equations for potential and kinetic energy of rigid body motion. The energy tracked throughout the event includes the kinetic energy in the moving roadbed, which represents the translation of a vehicle in a real world rollover.

The mass of the roadbed was maintained at 1633 kg for each JRS test, therefore the initial kinetic energy in the road was approximately equal for all tests. The propulsion system pulls the roadbed throughout the entire event, including during impact. The increase in kinetic energy, due to the

sustained propulsion, is calculated from a calibration (no-impact) run for each test (Figure 2). During the impact test the roadbed slows, but not as much as it would have if the propulsion had not been sustained. The increase in kinetic energy, calculated from the calibration run, is deducted from the measured kinetic energy during the impact test to produce an adjusted profile. The adjusted data was used in all energy calculations.

The roadbed approaches the impact zone on rollers but throughout impact it slides along lubricated skids during which time the roadbed slows due to friction. The amount of energy dissipated by friction during impact was estimated using the known coefficient of kinetic friction and the measured normal force on the road.

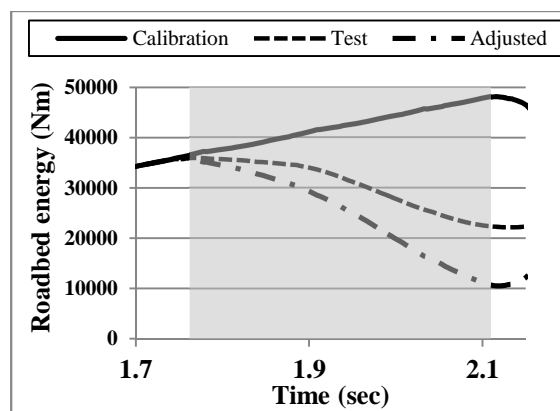


Figure 2. Roadbed energy profile for calibration test, impact test and adjusted result. Grey band indicates duration of vehicle to road impact.

The potential, vertical kinetic and rotational (roll and pitch) kinetic energy of each vehicle was calculated for the entire event. The potential energy of the vehicle was calculated using the distance between the CG of the vehicle and the roadbed, thus a vehicle in direct contact with the roadbed would have a non-zero potential energy. All rotational energy calculations were made assuming the rotation occurred about the appropriate axis passing through the centre of gravity and that the moments of inertia were constant. The sign convention used for the pitch motion, rotation about the lateral centre of gravity, is described in Figure 3. For an inverted vehicle the pitch is taken to be zero when horizontal and increases as the front moves nearer to the ground.

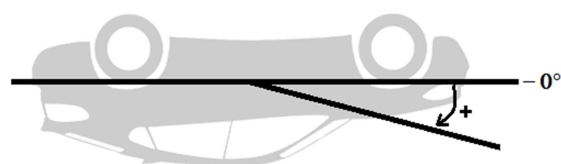


Figure 3. Pitch sign convention.

String potentiometers were used to measure the dynamic movement of the interior of the vehicle roof, relative to the approximate longitudinal centre of gravity (roll axis), at the top of each A-pillar, top of the far side B-pillar, and at the roof header approximately 200 mm inboard of the roof rail as shown in Figure 4. String potentiometers have been used in other dynamic rollover tests to measure dynamic roof movement [11, 12] and proved to provide accurate results. All test data was filtered at SAE channel frequency class 60, but the roof displacement data was further smoothed using a regularization method prior to being differentiated to obtain velocity and acceleration [13, 14]. This was done to reduce the amount of noise that is inherently amplified during numerical differentiation. The terms end of test (EOT) and residual will be used interchangeably throughout this paper to describe the amount of intrusion that is remaining at the end of the test. Roof intrusion is a decrease in the distance between the roof and the chassis. Peak dynamic intrusion is defined as the peak intrusion that occurs during an impact and is not necessarily the same as maximum intrusion which is the maximum amount of intrusion that occurred over a collection of impacts. For instance in a single roll event, where there is only 1 roof impact, the peak dynamic intrusion will be equal to the maximum intrusion. However in a two roll event with two roof impacts the maximum intrusion will be equal to the amount of residual intrusion from the first impact plus the peak dynamic intrusion from the second impact.

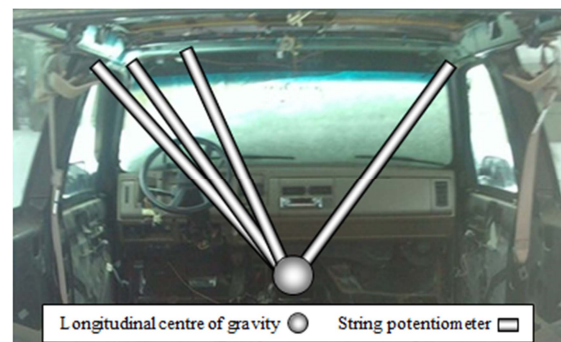


Figure 4. String potentiometer locations.

Two sections of results are presented below. The first, comprising roof intrusion data for all 48 vehicles, includes tests performed at a wide range of initial protocols. The second section, comprising vehicle kinematic and energy data for 21 vehicles, includes sequential tests performed at protocols A and B described in Table 1. The two differences between protocols A and B are the initial pitch angles and the fact that vehicles tested at protocol B had previously been tested once at protocol A.

**Table 1.**  
**Initial test conditions**

Pitch (A/B)	5° / 10°
Yaw	10°
Roll rate	180°/sec
Impact roll angle	145°
Road speed	6.7 m/s
Drop height	10.2 cm

The duration of the rollover event is defined as the time between first roof to ground impact and the time at which the vehicle is no longer in contact with the roadbed surface.

## RESULTS

### Roof Performance

The relationship between the maximum intrusion and the end of test intrusion was consistent for all vehicles, initial conditions, numbers of roof impacts and roof measurement locations. The scatter plot in Figure 5 was generated using 230 far side roof measurements from 83 various protocol JRS tests of 48 different vehicles. Equation 1, derived from the best fit line ( $R^2 = 0.96$ ) of the aggregated data, estimates the maximum amount of roof intrusion sustained during the event,  $y$ , from the known residual intrusion,  $x$ , as measured in centimetres. Occasionally the far side header experienced slight outward tenting during the near side impact which resulted in an overall negative residual intrusion value.

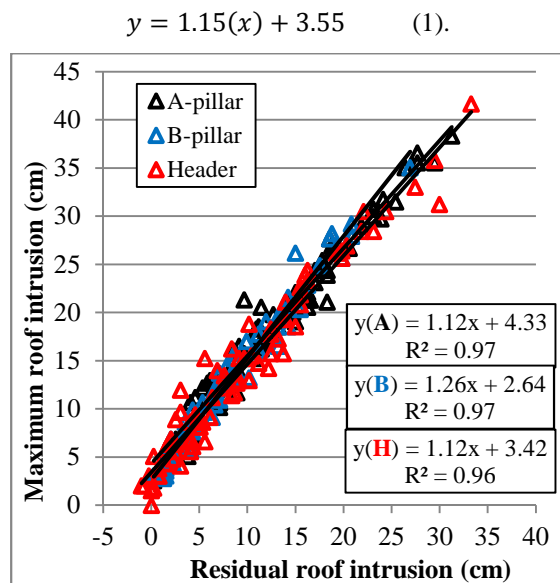


Figure 5. Residual roof intrusion vs. maximum intrusion by measurement location.

Similar results were obtained in inverted drop tests conducted by Batzer et al. [15] (Figure 6) and in curb trip tests [12]. The amount of maximum roof intrusion estimated by Equation 1 and the amount estimated by the inverted drop test data varied less than 5 cm over 40 cm of residual intrusion.

There was a moderate relationship between the peak speed at which the roof intruded during a roof to ground impact and the amount of dynamic intrusion that occurred, Figure 7.

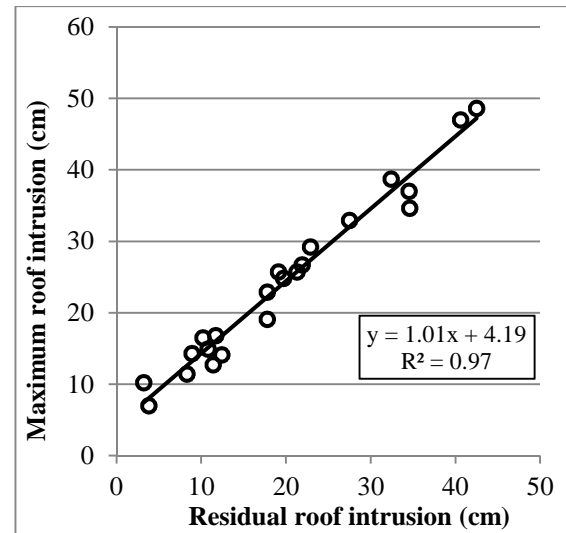


Figure 6. Residual roof intrusion vs. maximum roof intrusion in inverted drop tests after Batzer et al. [15]. Measurements taken at far side A-pillar, perpendicular to impact surface.

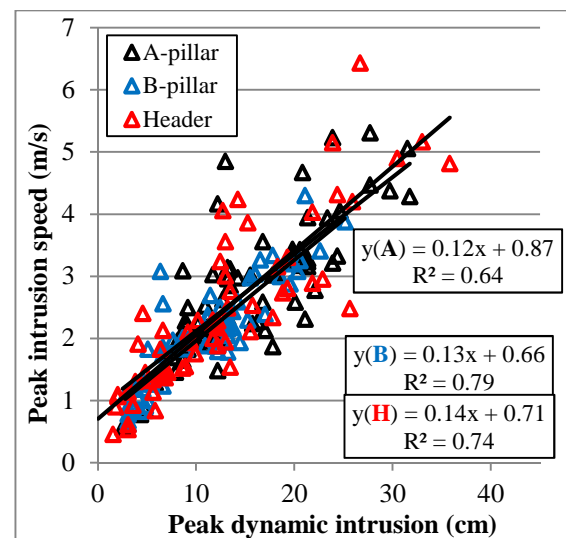


Figure 7. Peak dynamic roof intrusion vs. peak intrusion speed.

In general the peak acceleration of the intruding roof increased with increased peak dynamic intrusion, but the relationship was weak (Figure 8).

The peak acceleration was more closely related to the peak speed of roof intrusion, Figure 9. The relationships between all parameters in Figures 5-9 was strongest for measurements taken at the far side B-pillar.

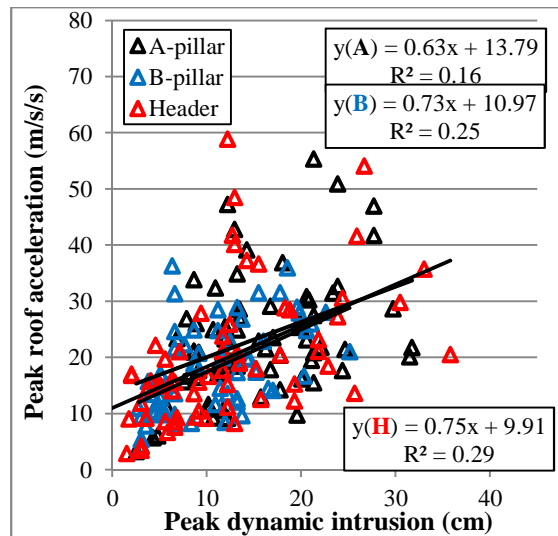


Figure 8. Peak dynamic roof intrusion vs. peak roof intrusion acceleration.

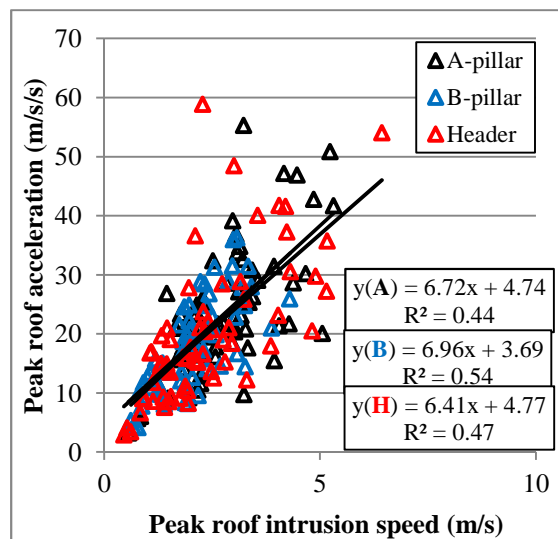


Figure 9. Peak roof intrusion speed vs. peak roof intrusion acceleration

### Vehicle Kinematics

The following results were obtained solely from tests conducted at protocols A and/or B. These tests were performed sequentially; therefore all vehicles tested at protocol B had previously been tested once at protocol A.

The total duration of impact varied between vehicles. It ranged from 0.389 to 0.294 seconds with an average of 0.347 seconds for test protocol

A. For test protocol B the duration of impact ranged from 0.404 to 0.272 seconds with an average of 0.333 seconds. On average the far side impact lasted 66.4 % longer than the near side impact for test protocol A and 33.6 % longer for test protocol B.

Two pitching modes were observed for vehicles tested at protocol A. The first mode, illustrated in Figure 10, consisted of the pitch generally increasing during the event until an impact between the road and far side front fender caused the pitch to stabilise. One example of the general vertical motion of the front and rear of the vehicle throughout the impact for the first pitching mode is shown in Figure 11. For this mode of pitching the front dropped at a constant rate as the rear remained at a fairly constant height. At far side impact the front continued to drop while the rear rose rapidly. When the front far side fender contacted the road, at approximately 210-235 degrees, the pitch stabilised as the vertical motion of the front and rear of the vehicle ceased. Contact between the vehicle and the road generally ended between 240 and 250 degrees of roll at which time the vehicles in this mode had pitch angle ranging from 8.7 to 12.4 degrees.

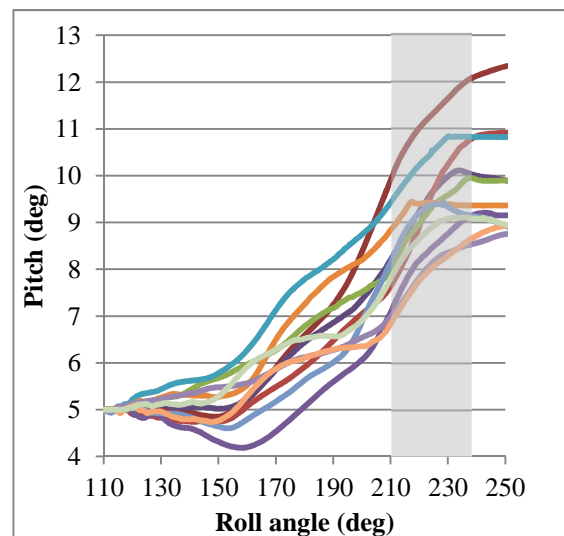


Figure 10. Roll angle vs. pitch for test protocol A. Pitching mode 1. Shaded area represents approximate start of fender contact. Each colour represents a separate test vehicle.

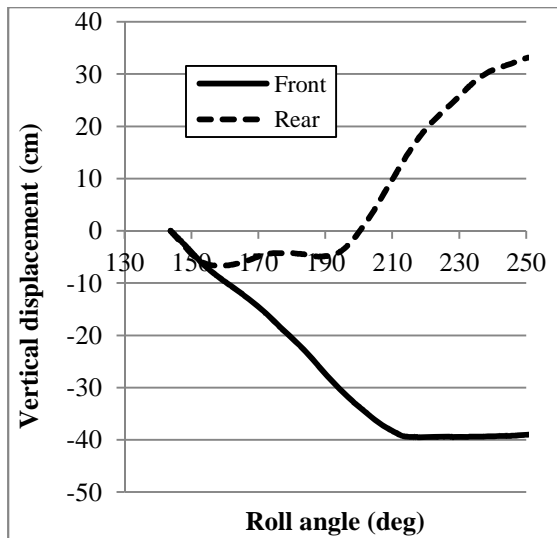


Figure 11. Roll angle vs. vertical displacement of front and rear of the vehicle. Test protocol A. Pitching mode 1.

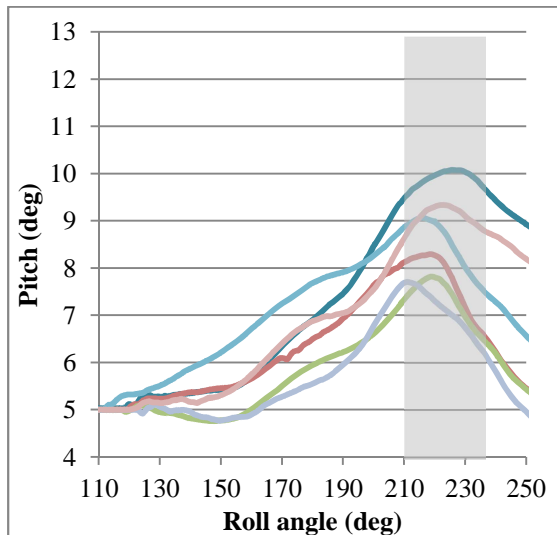


Figure 12. Roll angle vs. pitch for test protocol A. Pitching mode 2. Shaded area represents approximate start of fender contact. Each colour represents a separate test vehicle.

The overall pitch and the general motion of the front and rear of each vehicle in the second mode are shown in Figures 12 and 13 respectively. In this mode the pitch increased, to between  $7.6^\circ$  and  $10.1^\circ$ , up to the point of front far side fender contact at which point the pitch rate changed direction. At the time these vehicles left the roadway they were pitching at approximately  $-6.1^\circ$  per quarter turn. The vertical motion at the front and rear of the vehicle was similar to that of mode 1 up until far side roof impact. The impact between the far side of the roof and roadbed caused the rear of the vehicle to slowly move upwards with little effect on the motion of the front of the vehicle.

When the front far side fender contacted the roadbed the vertical motion of the rear of the vehicle was stopped while the front rapidly moved upward resulting in decreasing pitch. The range of pitch angles at far side impact for all vehicles was from  $3.4$  to  $8.1$  degrees.

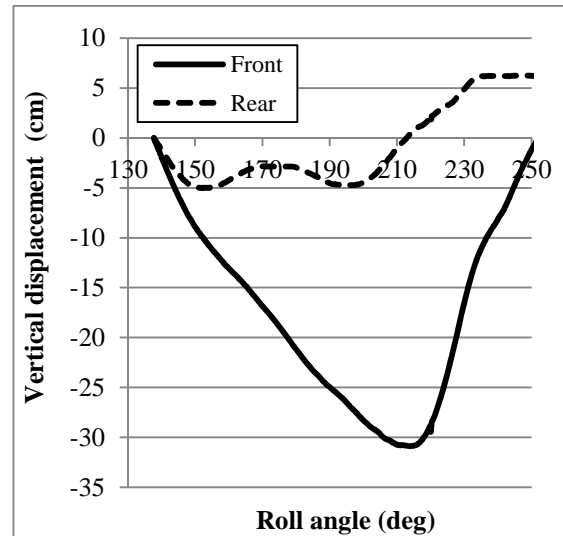


Figure 13. Roll angle vs. vertical displacement of front and rear of the vehicle. Test protocol A. Pitching mode 2.

For vehicles tested at protocol B the pitch response was generally similar, Figure 14. Most vehicles had a slightly increasing or stable pitch from initial impact through the far side roof contact and until front far side fender contact. Fender impact occurred earlier in the roll of test protocol B than test protocol A. The only major differences observed between each vehicle were the pitching motions resulting from far side fender contact. The motions ranged from abrupt changes in pitch, due to combined far side fender and roof contact, to cylindrical-type rolling with minor alterations in pitch angle. The range of pitch angles at far side impact was from  $7.8$  to  $11.9$  degrees. The pitch rates at the end of roadbed contact ranged from stable to  $-8.9^\circ$  per quarter turn.

Two different modes were identified for the vertical motion at the front and rear of the vehicle. The first mode, Figure 15, was characterised by minimal changes in overall pitch as the front and rear of the vehicle moved in tandem with one another. In the second mode, Figure 16, the front and rear of the vehicles generally fell together until far side roof and front fender impact at which point the front of the vehicle moved rapidly upward while the rear of the vehicle maintained its position.

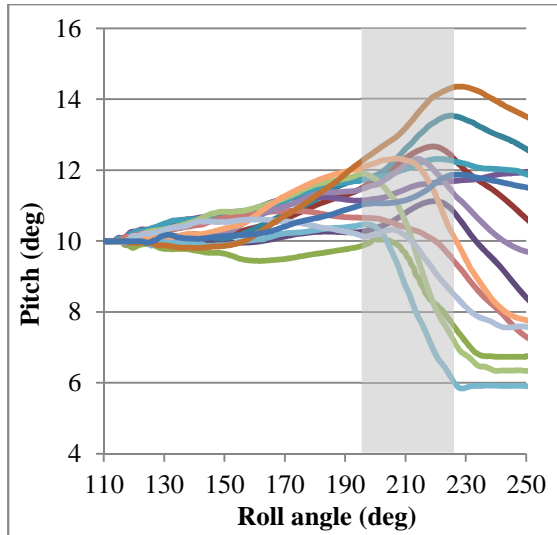


Figure 14. Roll angle vs. pitch for test protocol B. Shaded area represents approximate start of fender contact. Each colour represents a separate test vehicle.

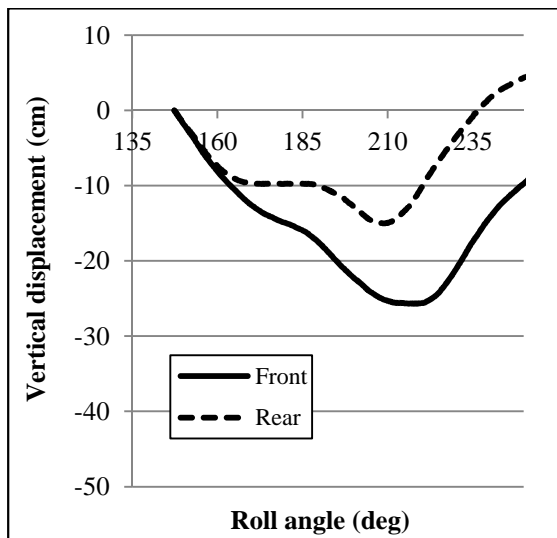


Figure 15. Roll angle vs. vertical displacement of front and rear of vehicle. Test protocol B. Pitching mode 1.

### Energy

The energy profiles at three instances in the rollover event for the tests performed at protocols A and B are shown in Figures 17 and 18. In each chart the first column for each vehicle, labelled with the name of the vehicle, describes the energy in the system just prior to initial impact. The second and third columns to the right describe the energy just prior to and just after far side impact, respectively. The difference between the total height of each column indicates the amount of energy dissipated during the event.

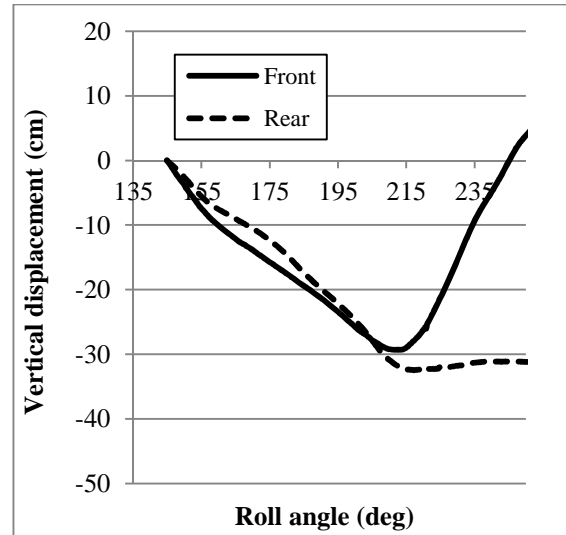


Figure 16. Roll angle vs. vertical displacement of front and rear of vehicle. Test protocol B. Pitching mode 2.

In some tests an increase in total energy was observed to occur during near side impact, e.g. compare the first and second column for the Volkswagen Tiguan in Figure 18. The increase in energy was on the order of 1 % of the total energy and was attributed to roll rate sensor noise.

A net energy loss was recorded for each vehicle during the rollover event. This loss was assumed to be due to the dissipation of energy in the form of friction between the roadbed and skids (calculation described in the methods section) and vehicle deformation. The average amount of energy dissipated during the near and far side impacts was 1.6 % and 19.9 % of the total initial energy for test protocol A, respectively. Of the energy dissipated in the far side impact, between 43.1 % and 84.2 % (average = 55.9 %) was estimated to have been in the form of vehicle deformation. For test protocol B the average amount of energy dissipated during the near and far side impacts was 2.7 % and 22.8% respectively. Of the energy dissipated in the far side impact, between 32.7 % and 75.5 % (average = 50.1 %) was estimated to have been in the form of vehicle deformation. The majority of the remaining energy was estimated to be lost due to friction between the roadbed and skids.

The amount of energy estimated to have been dissipated via far side roof deformation was related to the amount of peak dynamic roof intrusion that occurred during the event, Figure 19. This relationship was not as strong ( $R^2=0.35$ ) for test protocol B.

Figure 17. Energy profile for test protocol A. Note the vertical axis starts at 10,000 Nm.

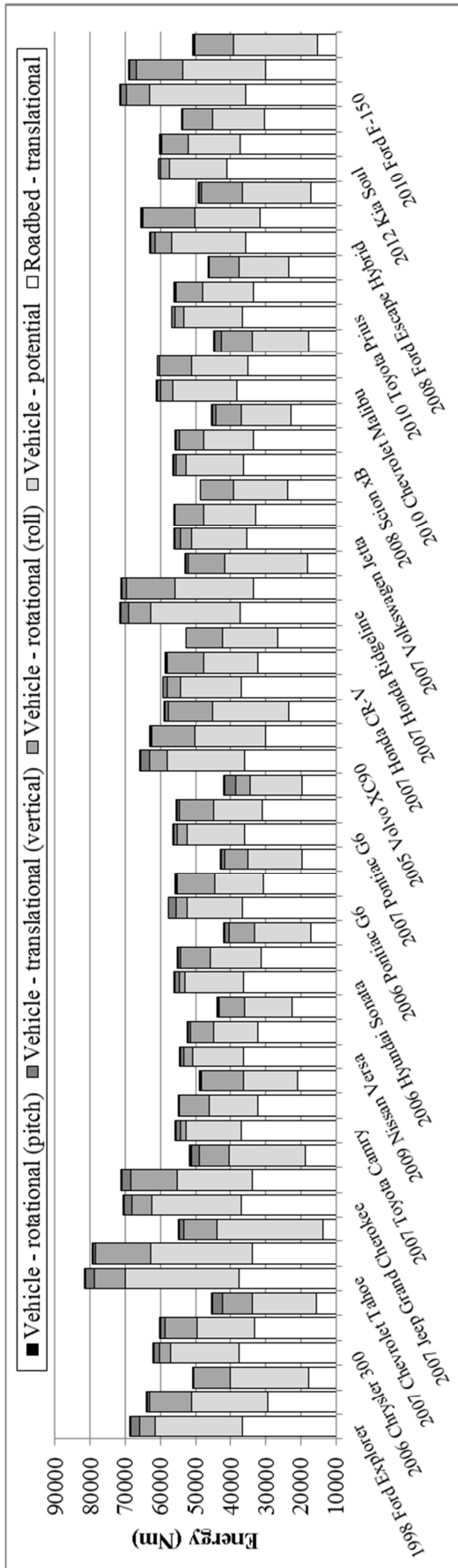
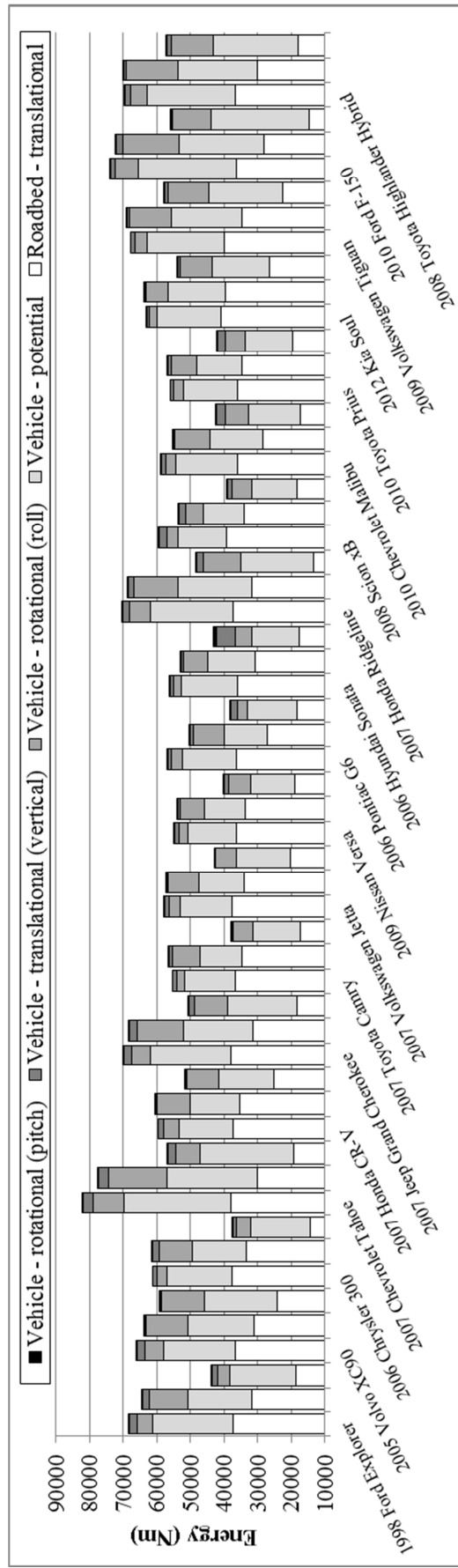


Figure 18. Energy profile for test protocol B. Note the vertical axis starts at 10,000 Nm.



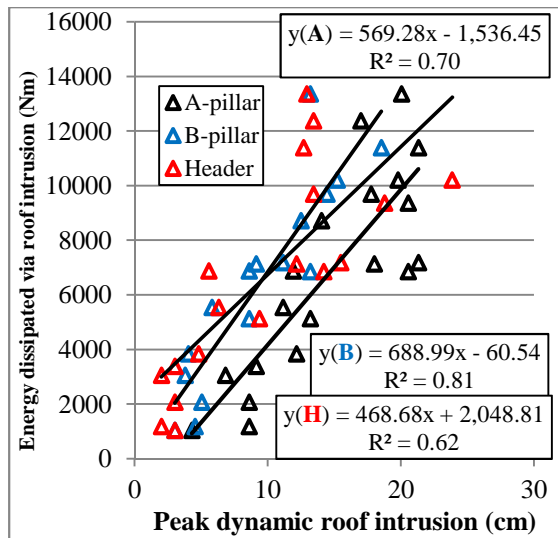


Figure 19. Peak far side dynamic roof intrusion vs. estimated energy dissipated by roof intrusion. Test protocol A.

Table 2 describes the change in energy that occurred throughout the entire event and during near and far side impacts for the three main forms of energy in the system. For each form of energy (roadbed translational, vehicle translational and vehicle rotational) the total range and average per cent change is listed. Overall there was little difference between the transformation of energy in test protocols A and B. The general trend was that the overall translational energy of the roadbed and vehicle decreased while the rotational energy of the vehicle increased. For all vehicles in each test the roadbed slowed during the near and far side impacts. In both test protocols every vehicle lost vertical kinetic and potential energy during near side impact as its vertical motion was slowed due to impact with the road. At far side impact, however, vehicles generally bounced upward causing an increase in the vertical translational energy. On average vehicles tended to end the roll event with less vertical translational energy than they had initially. The near side impact resulted in an increase in rotational energy for every vehicle in every test. For test protocol A the change in a vehicle's rotational energy during far side impact was related to the amount of peak dynamic far side roof deformation, Figure 20. Vehicles with low amounts of intrusion experienced an increase in rotational energy while those with greater amounts of intrusion experienced a decrease in rotational energy. For test protocol B all but one vehicle either maintained or lost rotational energy. There was no relationship between the change in rotational energy and roof intrusion. The amount of energy in the vehicle's pitching motion was less than 1% of the total energy in the system throughout the rollover event.

Table 2. Per cent change in energy for three forms of energy.

	Roadbed translational		Vehicle translational		Vehicle rotational	
	Range	Average	Range	Average	Range	Average
Roll 1	-63.9 – -25.9	-45.1	-17.7 – 2.2	-9.9	6.6 – 271	139.9
Near side	-23.1 – -7.8	-15.5	-18.2 – -7.1	-13.5	90.6 – 261	171.4
Far side	-59.7 – -17.5	-37.6	4.1 – 20.2	5.3	-55.5 – 42.7	-8.9
Roll 2	-64.7 – -32.4	-49.2	-18 – 11.2	-7.3	-23.1 – 288	101.8
Near side	-25.8 – -9.7	-16	-19.6 – -9.3	-14.5	76.2 – 243	158.9
Far side	-58.4 – -23.0	-41.3	-0.1 – 35.3	9.5	-68.9 – 44.4	-23.6

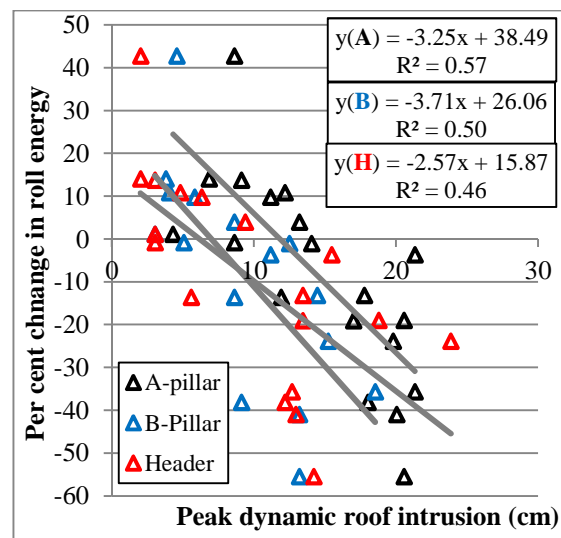


Figure 20. Peak dynamic roof intrusion vs. per cent change in roll energy during far side impact. Test protocol A.

## DISCUSSION

Strong relationships were observed between maximum and residual roof intrusion and moderately strong relationships between peak dynamic intrusion and peak intrusion speed. These relationships were always strongest for measurements taken at the far side B-pillar. This is believed to be due to the greater stiffness and alignment of the B-pillar as compared to that of the A-pillar and header. While peak intrusion speed was moderately related to the peak intrusion acceleration, peak dynamic intrusion had a very weak relationship with acceleration. This may be due to the method of calculating speed and acceleration from displacement where a single differentiation step (i.e. between displacement and speed or between speed and acceleration) would maintain any relationship while the two differentiation steps between displacement and acceleration might have amplified enough of the noise to weaken the relationship. Further, differences in roof elasticity and the time at which glazing failed would have an effect on the relationship.

The major difference between the pitching modes observed for protocol A was the effect of far side front fender impact. Vehicles with more volatile pitch (mode 2) had relatively long front bonnets, with respect to their overall length, and a generally lower profile. They also had an average of 52 % more peak dynamic roof intrusion at the A-pillar and 47.6 % more at the B-pillar than vehicles exhibiting behaviour consistent with mode 1. Similarly, the vehicles grouped in the second mode for test protocol B had more severe pitching motion than those in mode 1 and were relatively weaker and longer. The average SWR for mode 2 vehicles was 3.1 compared to 4.3 and they experienced 34.5 % to 70 % more roof intrusion at the A and B pillars, respectively. The vehicles in mode two were an average of 30.5 cm longer than those in mode 1.

The results of the pitching motion highlight the wide range of vehicle kinematics that can occur during the roof impact phase of a rollover due to differences in vehicle shape and roof strength. This difference adds to the complexity of establishing a protocol, considering both vehicle and ATD initial conditions, for a second test.

The energy profiles for all tests had many similarities. The roadbed lost energy throughout the event and the vehicle gained energy in the form of rotational velocity during the near side contact. The increase in roll rate during near side contact was due to the difference in peripheral velocity of the vehicle and translational velocity of the roadbed.

The change in rotational energy during far side impact for test protocol A was dependant on the amount of roof intrusion that occurred. With one exception, the roll rate at far side impact for test protocol B either remained constant or decreased. This was due to the more severe fender contact that occurred with greater pitch angles.

The difference in vehicle performance can be seen in Figures 17 and 18. Vehicles which had low amounts of roof intrusion, such as the Volvo XC90 and Honda CR-V had relatively small amounts of energy lost during near and far side impacts. These vehicles nearly maintained their roll energy through the final impact while the roadbed lost energy gradually. On the other hand vehicles like the Chevrolet Tahoe and the Jeep Grand Cherokee had relatively large losses in energy during the far side impact. The high levels of roof intrusion in these vehicles during the far side impact resulted in great losses in vehicle rotational and roadbed translational energy.

Although the initial conditions of the tests for respective protocols were the same the initial energy was different for each vehicle due to the differences in vehicle size. The amount of initial roll, potential or total energy did not appear to be related to the performance of the roof during the event.

During each test approximately 8-17 % of the total system energy was dissipated via work done deforming the vehicle body. A moderate relationship was found between peak dynamic roof intrusion and energy dissipated via vehicle deformation for test protocol A. The relationship was strong for test protocol A because roof deformation accounted for the majority of vehicle damage. This was not the case for test protocol B in which significant fender to road contact would have resulted in dissipation of energy that would not have been accounted for in roof deformation measurements.

## CONCLUSIONS

In tests performed on the JRS at the stated protocols a few relationships were observed. The amount of maximum roof intrusion could be accurately predicted for known amounts of residual roof intrusion using Equation 1. Peak roof intrusion speed is related to, but not fully predicted by, peak dynamic intrusion. Peak roof intrusion speed is moderately related to the peak acceleration of the roof during impact. The resulting pitch motion of a vehicle appears to be related to its geometry and roof performance. The kinetic and potential energy in the roadbed and vehicle could be tracked throughout each JRS test. The amount of energy

dissipated via friction and vehicle deformation could be estimated for each test. For test protocol A the estimated amount of energy dissipated via roof deformation correlated fairly well with the amount of roof intrusion.

## ACKNOWLEDGEMENTS

The authors would like to thank the Australian federal government's Australian Research Council for providing funds to carry out this research through the Linkage Projects grants scheme (No: LP110100069). The authors would also like to thank the industry partners for also providing the Partner Organisation funding, namely, the New South Wales state government's Centre for Road Safety, the Victorian state government's 3rd party insurer Transport Accident Commission (TAC), the West Australian (WA) state government's Office of Road Safety at Main Roads WA, the mining company BHP Billiton Ltd, and the US Center for Injury Research (CFIR). CFIR is also gratefully acknowledged for supplying the JRS test data.

## REFERENCES

- [1] G.A. Mattos, R. Grzebieta, M. Bambach, and A.S. McIntosh, *Validation of a dynamic rollover test device*, Int. J. Crashworthiness (2013).
- [2] M.L. Brumbelow, E.R. Teoh, D.S. Zuby, and A.T. McCartt, *Roof strength and injury risk in rollover crashes*, Traffic Inj. Prev. 10 (2009), pp. 252-265.
- [3] M.L. Brumbelow and E.R. Teoh, *roof strength and injury risk in rollover crashes of passenger cars*, Traffic Inj. Prev. 10 (2009), pp. 584-592.
- [4] K.F. Orłowski, R.T. Bundorf, and E.A. Moffatt, *Rollover crash tests - the influence of roof strength on injury mechanics*, 1985, Society of Automotive Engineers: Warrendale, PA. p. 181-203.
- [5] G.S. Bahling, R.T. Bundorf, G.S. Kaspzyk, E.A. Moffatt, K.F. Orłowski, and J.E. Stocke, *Rollover and drop tests - The influence of roof strength on injury mechanics using belted dummies*, in Stapp Car Crash Conference 1990, Society of Automotive Engineers: Warrendale, PA. p. 101-112.
- [6] R. Grzebieta, M. Bambach, A. McIntosh, K. Digges, S. Job, D. Friedman, K. Simmons, E.C. Chirwa, R. Zou, and F.A. Pintar, *The dynamic rollover protection (DROP) research program*, Proc. 8th International Crashworthiness Conference, Milan, Italy, 2012.
- [7] J. Bish, J. Caplinger, D. Friedman, A. Jordan, and C. Nash, *Repeatability of a dynamic rollover test system*, Proc. International Crashworthiness Conference Kyoto, Japan, 2008.
- [8] E.C. Chirwa, R.R. Stephenson, S.A. Batzer, and R.H. Grzebieta, *Review of the Jordan Rollover System (JRS) vis-a-vis other dynamic crash test devices*, Int. J. Crashworthiness 15 (2010), pp. 553-569.
- [9] A. Jordan and J. Bish, *Repeatability testing of a dynamic rollover test fixture*, Proc. 19th International technical Conference on the Enhanced Safety of Vehicles, Washington, DC, 2005.
- [10] J.R. Kerrigan, A. Jordan, D. Parent, Q. Zhang, J. Funk, N.J. Dennis, B. Overby, J. Bolton, and J. Crandall, *Design of a dynamic rollover test system*, SAE International Journal of Passenger Cars - Mechanical Systems 4 (2011), pp. 870-903.
- [11] G. Rains and M.A. Van Voorhis, *Quasi static and dynamic roof crush testing*, 1998, NHTSA, Vehicle Research and Test Center: Washington D.C.
- [12] S.W. Harvin, B.M. O'Brien-Mitchell, A.R. Dwoinen, C.A. Nassoioy, D.F. Motowski, A.G. Melocchi, H. Lu, and M.V. Peace, *Evaluation of Dynamic Roof Deformation in Rollover Crash Tests*, SAE International Journal of Passenger Cars - Mechanical Systems 4 (2011), pp. 807-829.
- [13] J.J. Stickel, *Data smoothing and numerical differentiation by a regularization method*, Computers & Chemical Engineering 34 (2010), pp. 467-475.
- [14] P.H.C. Eilers, *A Perfect Smoother*, Analytical Chemistry 75 (2003), pp. 3631-3636.
- [15] S.A. Batzer and R.M. Hooker, *Dynamic roof crush intrusion in inverted drop testing*, Proc. 19th ESV Conference, Washington, D.C. , 2005.